Examining the application and Usefulness of the Tasseled Cap Transformation and the Normalized Differential Vegetation Index to Multitemporal Imagery.

Submitted by Charles Buniger

Abstract

The LandSAT missions have faithfully provided time series remotely sensed data for many decades and continue to this day with the LandSAT-8 Operational Land Imager mission. This data has been widely disseminated and has provided the basis for effective Land and Hydrological management practices. Classifying and monitoring the amount and vigor of vegetative growth is one aspect of effective land and hydrological management that the Tasseled Cap Transformation (TCT) and Normalized Difference Vegetation Index (NDVI) contribute greatly to. This report used both of these tools to examine LandSAT-8 data over one growing season and conclude that both the TCT and NDVI provide complementary products for identifying, quantifying, and classifying data. The usefulness of the TCT and NDVI products diverge according to the intended end use in that the TCT maintains greater dimensionality for additional classification or study whereas the NDVI compresses and flattens the data, lending itself to be readily statistically parsed or used in the map creation process.

Data Sources

The imagery used for this project consists of three alternate months of LandSAT 8 Operational Land Imager (OLI) data. The time series begins in May 2018 and ends September 2018. This data was downloaded from the USGS Earth Explorer website April 27th, is processed to Level- 1T (Terrain Corrected) and provided in the GeoTIFF format. The Level-1T processing level provides data with the following data characteristics: 30 meter multispectral/ 15 m panchromatic pixel size, Universal Transvere Mercator (UTM) map projection, World Geodetic System (WGS) 84 datum, 12 m circular error, 90% global accuracy for OLI, and 16-bit unsigned pixel values.[1] The LandSAT-8 OLI sensor is comparable to that of its predecessor the Enhanced Thematic Mapper but includes two additional channels: the deep blue band 0.443 ųm for coastal and aerosol observations and the cirrus band at 1.375 ųm for cloud detection.[2] The OLI Focal Plane Array consists of 14 Focal Plane Modules made up of Silicone detectors for visible and Near Infrared bands and Mercury Cadmium Tellurium detectors for the short wave infrared bands. These sensors collect reflected solar energy, convert this to radiance, and rescale this data to a 16-bit Digital Number (DN) with values from 0 to 65536.[2]

The area under consideration is located in WRS2 Path 34, Row 34. This area is located in South Central Colorado and is characterized by mountainous terrain primarily above 8500 feet Mean Sea Level. The very large San Luis Valley that is home to a robust farming community is located towards the left edge of the LandSAT scene. The local farmers in the area grow potatoes and alfalfa which are both fairly intensive crops and require maintenance, potatoes more so than alfalfa. The data for this study was subset to include the valley floor for image processing and further subset to include only the agricultural areas for studying the methods of vegetative quantification.

Process

The imagery selected for this project was specifically chosen to capture the growing season at the beginning, middle and end in an attempt to identify the stages of growth. Once the imagery was loaded

into the ERDAS Imagine environment the Digital Numbers for the entire scene were converted to Top of Atmosphere (ToA) reflectance values using the spatial modeler formula for this function:

$$R_l' = M_l Q_{cal} + A_r$$

Where:

R_l' = TOA planetary reflectance without correction for solar angle.

M_l = Band-specific multiplicative rescaling factor from the metadata

Q_{cal} = Quantized and calibrated standard product pixel values (DN)

A_r = Band-specific additive rescaling factor from the metadata

TOA reflectance is corrected for the sun angle by:

$$R_l = r_l' / \sin(\text{solar elevation angle})$$

Where:

R_l = TOA planetary reflectance

R_l' = product of TOA reflectance without correction

Solar Elevation angle = local sun elevation from the metadata

The model for this conversion was downloaded from the Hexagon Geospatial tutorial website and is shown in figure 1 below.[3]

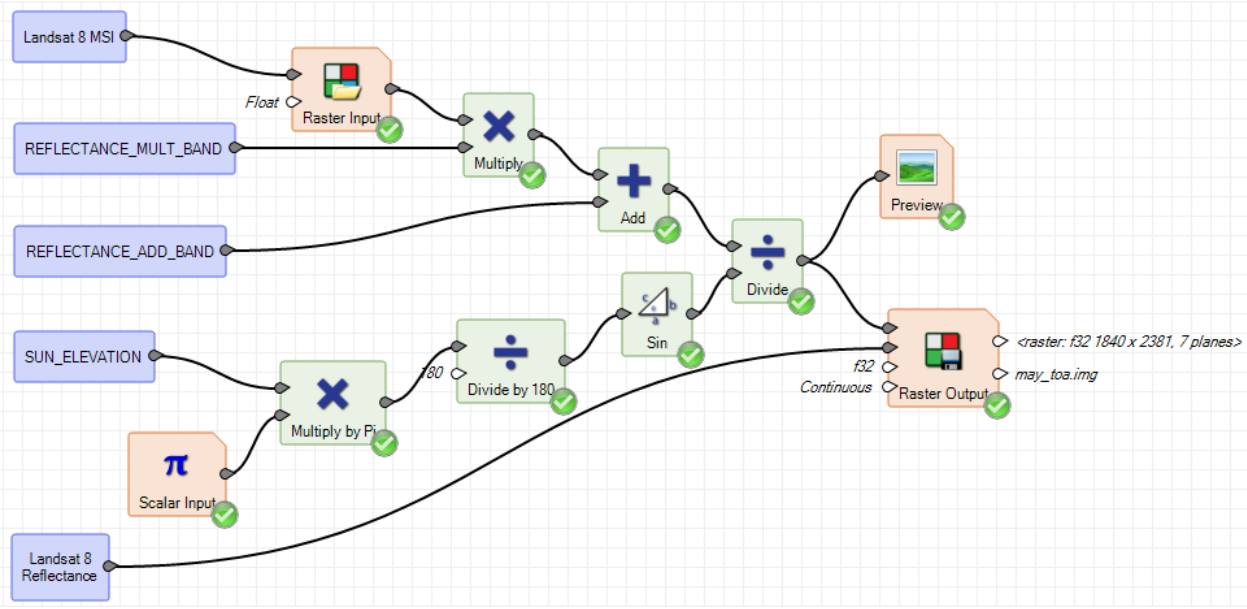

Figure 1: Spatial model flowchart for converting DN values to ToA radiance. Courtesy of Hexagon Geospatial.

The individual image files read by ERDAS for each month are comprised of a layer stack that contains the seven individual bands. This format enables the reordering of the bands for display and for processing functions to be executed with the information in the correct order. The flowchart in figure 2 shows the additional steps that were undertaken for atmospheric correction and image sub-setting to isolate relevant spectral information.

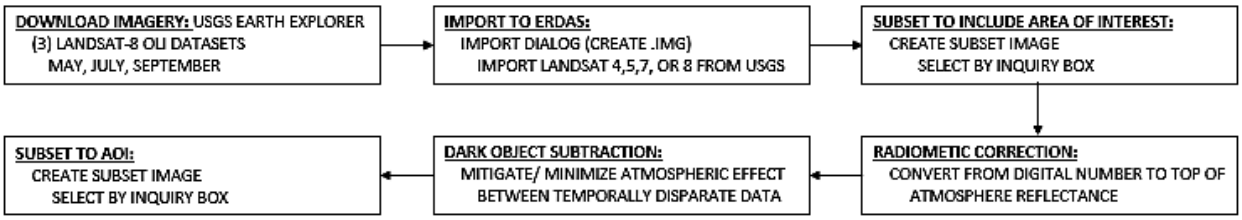

Figure 2: Flowchart depicting preprocessing steps taken prior to creating the Tasseled Cap and NDVI products.

To allow comparisons between datasets acquired at different times to be made the Dark Object Subtraction method of atmospheric correction was employed. This approach estimates the effect the atmosphere has on the data collected by the sensor by determining the average value for a dark area of the image and subtracting that value from the ToA reflectance values of the entire image. This process uses the "rationale that the only possible source for an observed signal from a dark object is the path radiance" and that this effect will be common, but different, among all images.[4] The flowchart for this process and the values employed for the correction are shown in figures 3 and 4. A small lake located in the Area of Interest (AOI) was used to determine the DOS values.

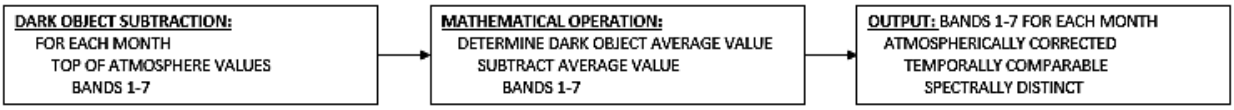

Figure 3: Flowchart showing steps taken to correct for different atmospheric conditions between datasets allow multitemporal comparisons between datasets to be made.

	MAY					JULY					SEPTEMBER				
	SAMPLED VALUES				AVG	SAMPLED VALUES				AVG	SAMPLED VALUES				AVG
BAND 1	0.087776	0.087933	0.087531	0.088089	0.087832	0.099973	0.100018	0.099973	0.100625	0.100147	0.084928	0.085339	0.084619	0.085236	0.085031
BAND 2	0.069739	0.069493	0.069761	0.070654	0.069912	0.080711	0.08015	0.080194	0.082082	0.080784	0.065741	0.066744	0.064712	0.065818	0.065753
BAND 3	0.056992	0.055162	0.060497	0.063042	0.058923	0.064214	0.064102	0.063675	0.068574	0.065141	0.051054	0.054115	0.050129	0.051852	0.051787
BAND 4	0.048777	0.045518	0.051009	0.054023	0.049832	0.04938	0.049762	0.049784	0.051155	0.05002	0.043236	0.044444	0.043081	0.039197	0.04249
BAND 5	0.017189	0.018596	0.018171	0.017904	0.017965	0.047132	0.040659	0.036254	0.053942	0.044497	0.059311	0.043493	0.039506	0.051415	0.048431
BAND 6	0.009063	0.010023	0.008907	0.00913	0.009281	0.007912	0.007912	0.008001	0.008361	0.008046	0.005684	0.005556	0.006687	0.005658	0.005896
BAND 7	0.006898	0.007456	0.006318	0.00692	0.006898	0.004653	0.004877	0.00481	0.005147	0.004872	0.004038	0.00427	0.005324	0.003884	0.004379

Figure 4: Values used to perform the Dark Object Subtraction.

Now that the data has been converted to Top of Atmosphere radiance values and adjusted to facilitate comparison the execution of the Tasseled Cap Transformation and creation of the Normalized Differential Vegetation Index can proceed. By applying weighted sums to every band in the stack, the Tasseled Cap Transformation (TCT) is a fixed model that rotates and condenses the spectral space so that most of the information is contained in the first two components, brightness and greenness. Brightness is "defined in the direction of the principal variation in soil reflectance". Greenness is "approximately orthogonal to brightness and is a contrast between the NIR and visible bands".[3] The flowchart below illustrates the steps each LandSAT scene underwent to produce the TCT product. The process flowchart used by ERDAS to calculate the TCT is included in the appendix following this report.

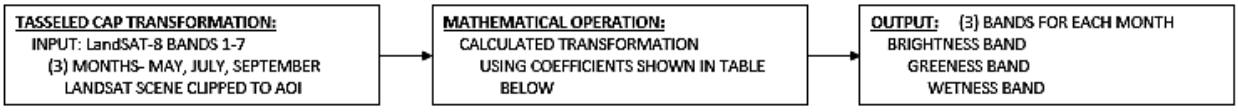

Figure 5: TCT transformation flowchart showing basic steps taken to implement the transformation

	LS 8 Band 1	LS 8 Band 2	LS 8 Band 3	LS 8 Band 4	LS 8 Band 5	LS 8 Band 6	LS 8 Band 7
Brightness	0.0000	0.3029	0.2786	0.4733	0.5599	0.5080	0.1872
Greenness	0.0000	-0.2941	-0.2430	-0.5424	0.7276	0.0713	-0.1608
Wetness	0.0000	0.1511	0.1973	0.3283	0.3407	-0.7117	-0.4559
TCT4	0.0000	-0.8239	0.0849	0.4396	-0.0580	0.2013	-0.2773
TCT5	0.0000	-0.3294	0.0557	0.1056	0.1855	-0.4349	0.8085
TCT6	0.0000	0.1079	-0.9023	0.4119	0.0575	-0.0259	0.0252

Figure 6:Coefficients used for the TCT. Courtesy of Hexagon Geospatial user community.[6]

To eliminate statistical influence from the material in the area that is not agriculturally related an inquiry box was established in the middle of the valley.

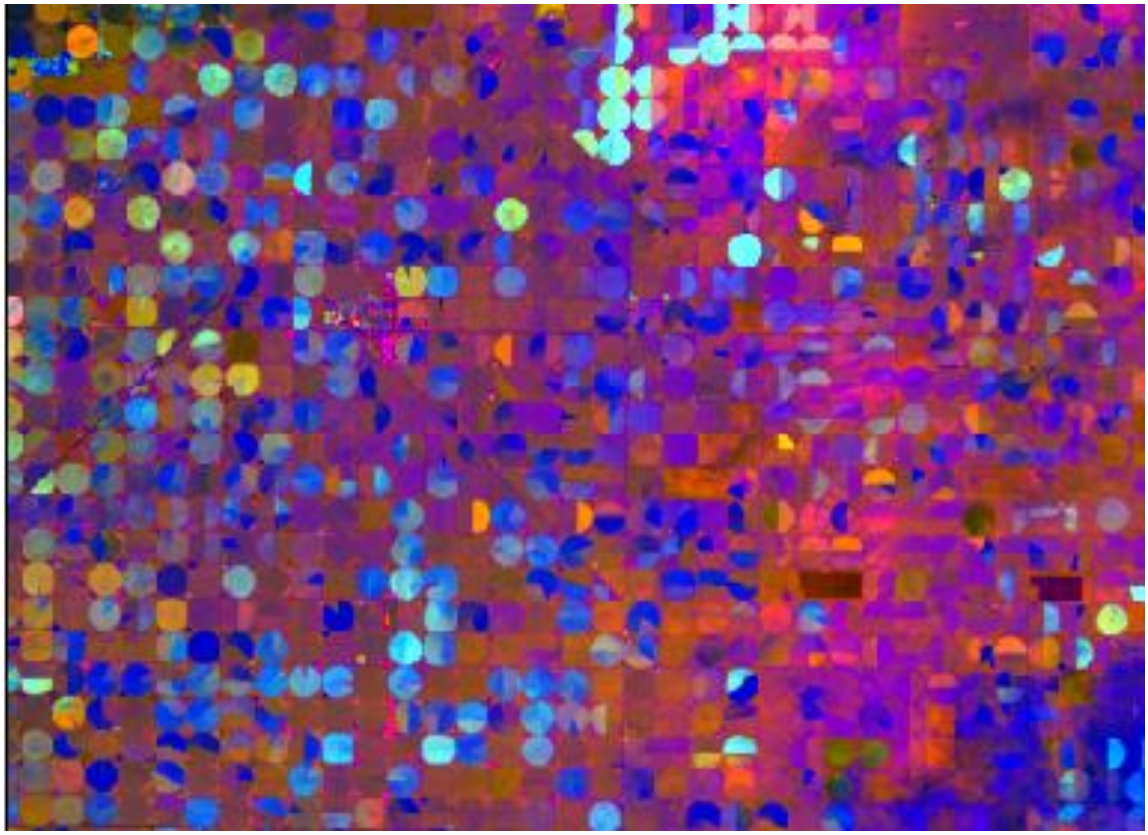

Figure 7: TCT product from May 2018 displayed as RGB→ Brightness, Greenness, Wetness

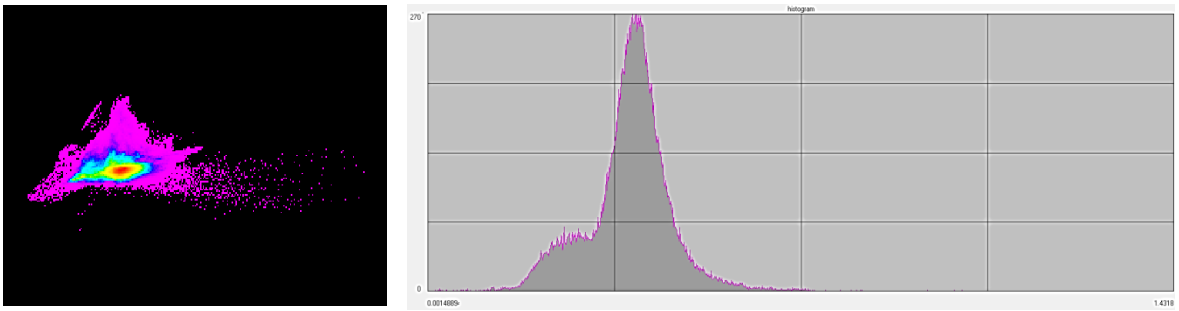

Figure 8: May 2018 TCT Scatterplot (Brightness vs. Greenness) and Histogram

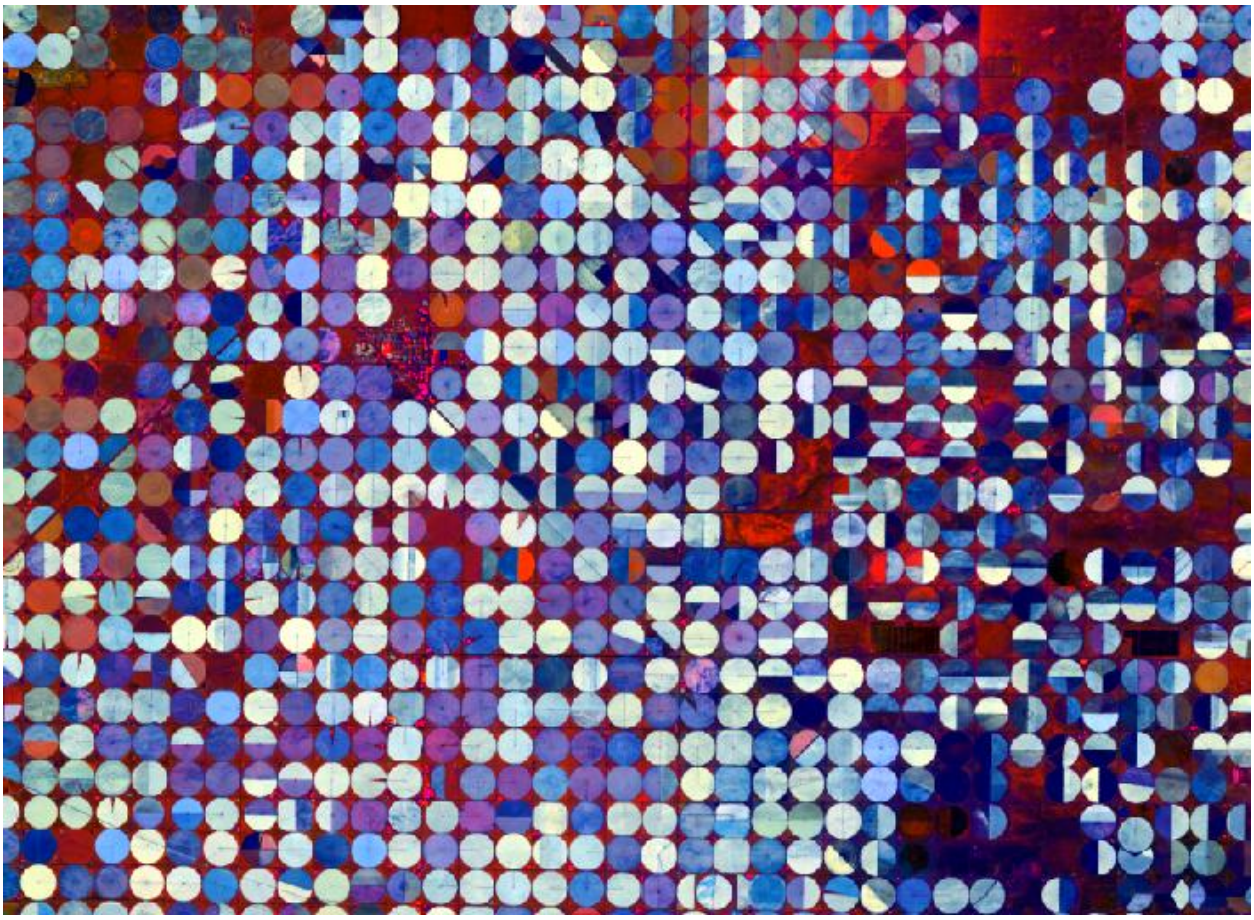

Figure 9: TCT product from July 2018 displayed as RGB→ Brightness, Greenness, Wetness

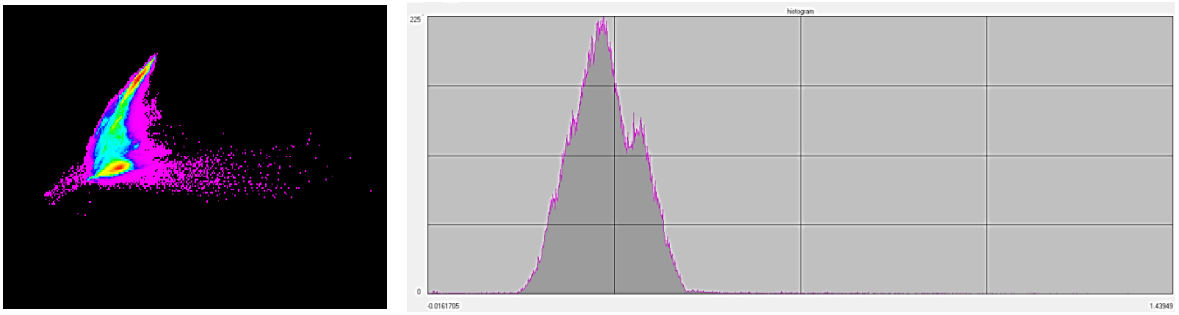

Figure 10: July 2018 TCT Scatterplot (Brightness vs. Greenness) and Histogram

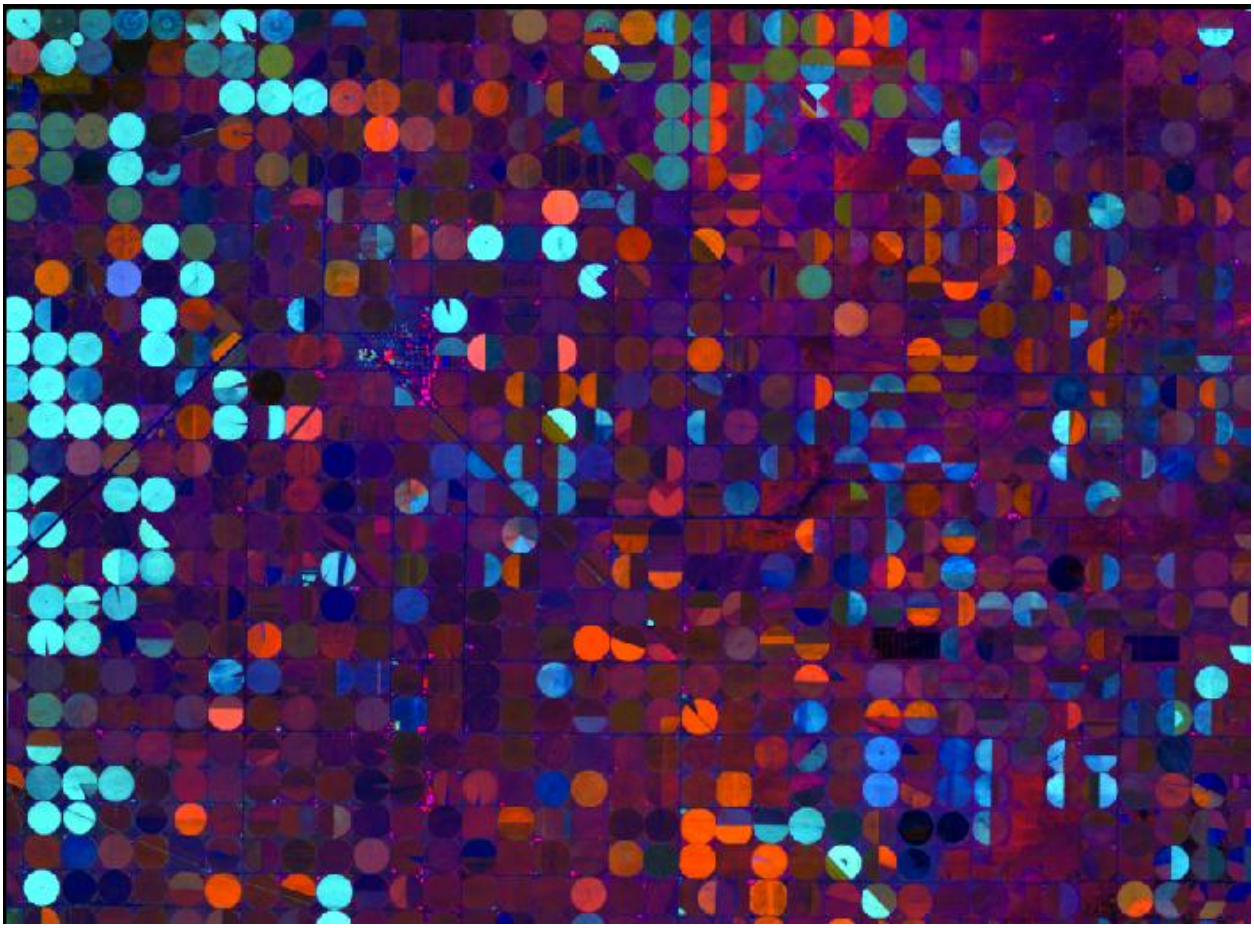

Figure 11: TCT product from September 2018 displayed as RGB→ Brightness, Greenness, Wetness

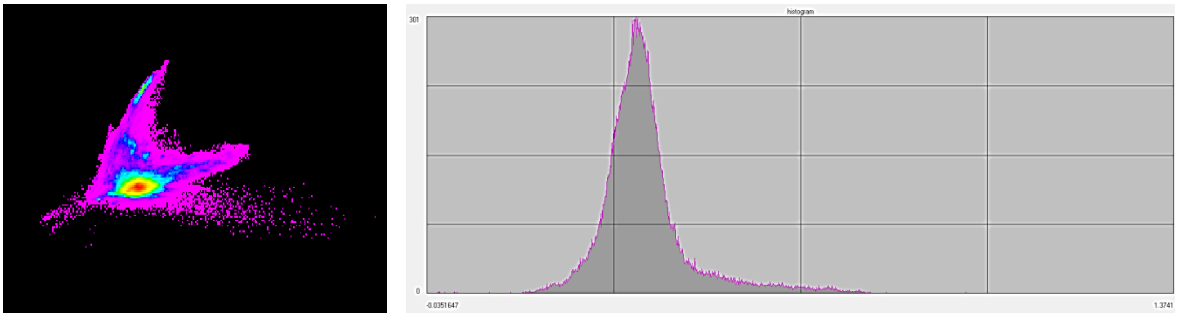

Figure 12: September 2018 TCT Scatterplot (Brightness vs. Greenness) and Histogram

The rotation and scaling of the spectral bands very clearly increases the separability between scene constituents which has the practical effect of this transformation is visually striking and allows for very rapid interpretation and rudimentary quantification.

Following the calculation of the TCT, the Normalized Differential Vegetation Index (NDVI) was calculated from the red and near infrared bands. The result is a dimensionless index with values that range from -1 to 1. These values are higher for healthy vegetation and lower in areas of sparse

vegation.[8] The NDVI creation process rejected all attempts made with the data that had undergone Dark Object Subtraction, so the original uncorrected data was utilized to generate the following NDVI products. The equation for calculating NDVI is shown in the flowchart in figure 19.

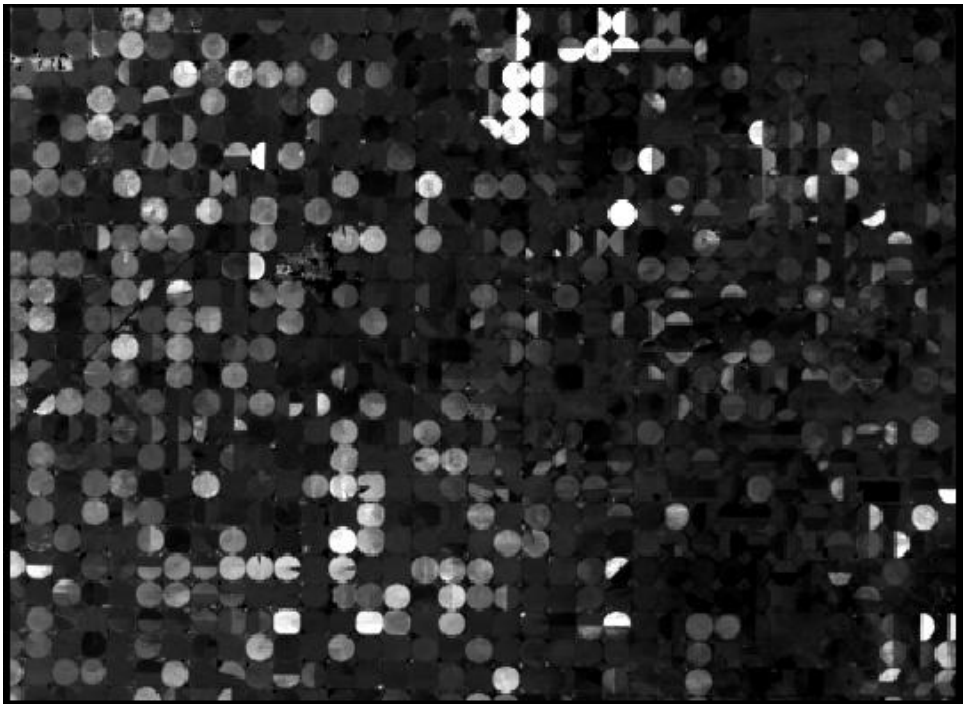

Figure 13: NDVI product from May 2018

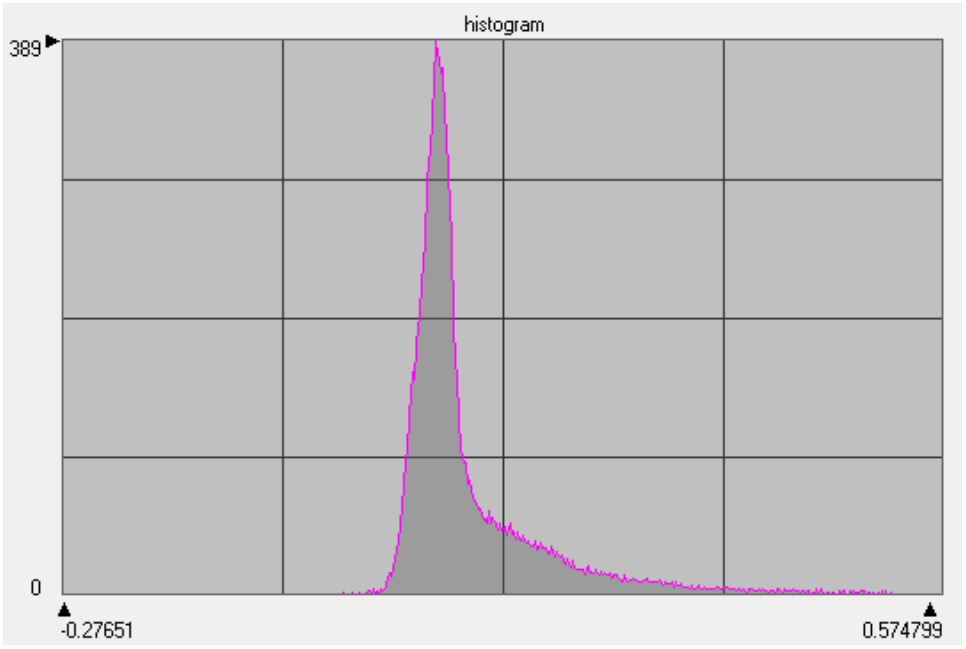

Figure 14: Histogram of NDVI product from May 2018

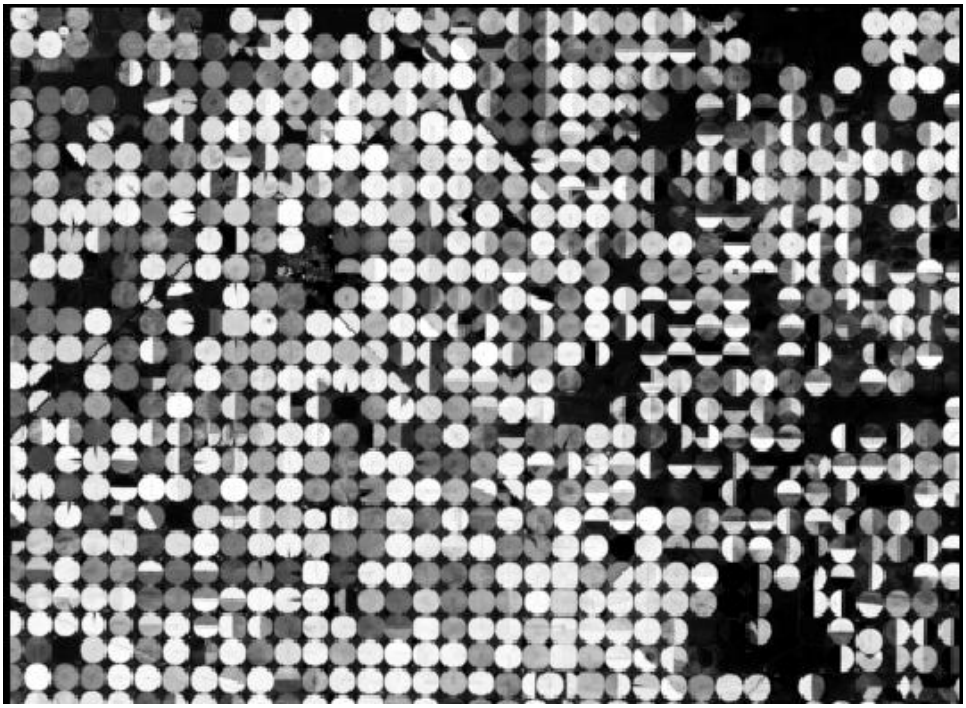

Figure 15: NDVI product from July 2018

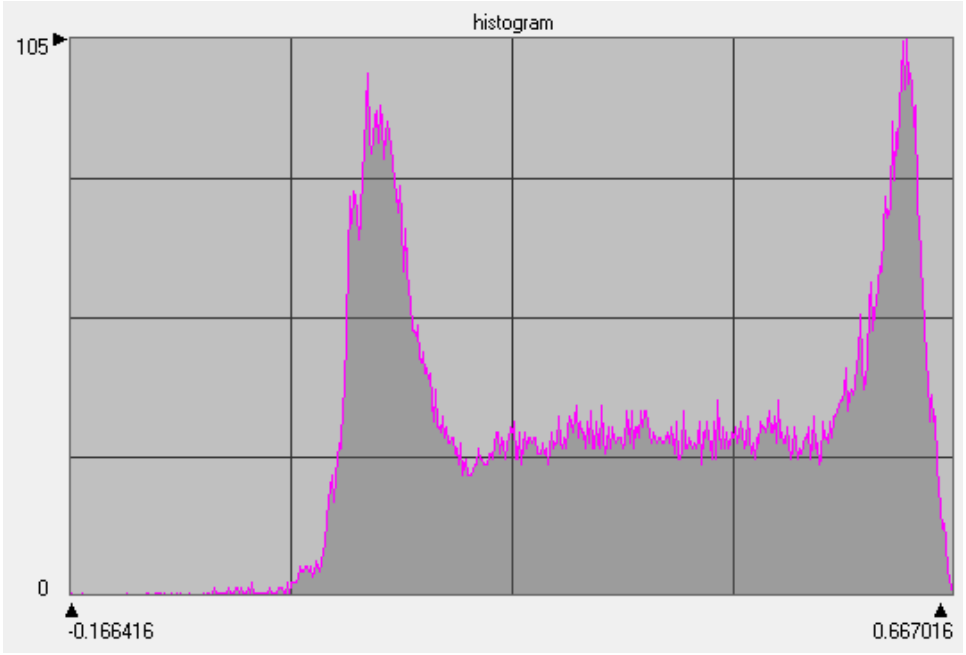

Figure 16: Histogram of NDVI product from July 2018

As a measure of vegetative land cover the "NDVI is preferred for global vegetation monitoring because the NDVI helps compensate for changing illumination conditions, surface slope, aspect, and other extraneous factors"[5] that affect multitemporal datasets with large, often discontinuous, spatial extents.

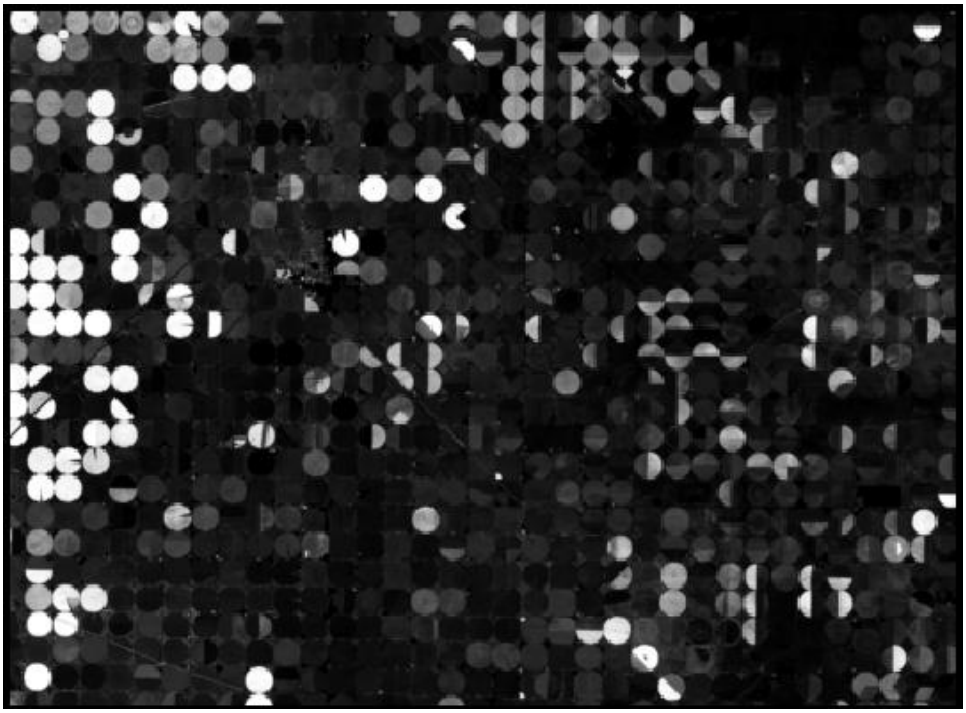

Figure 17: NDVI product from September 2018

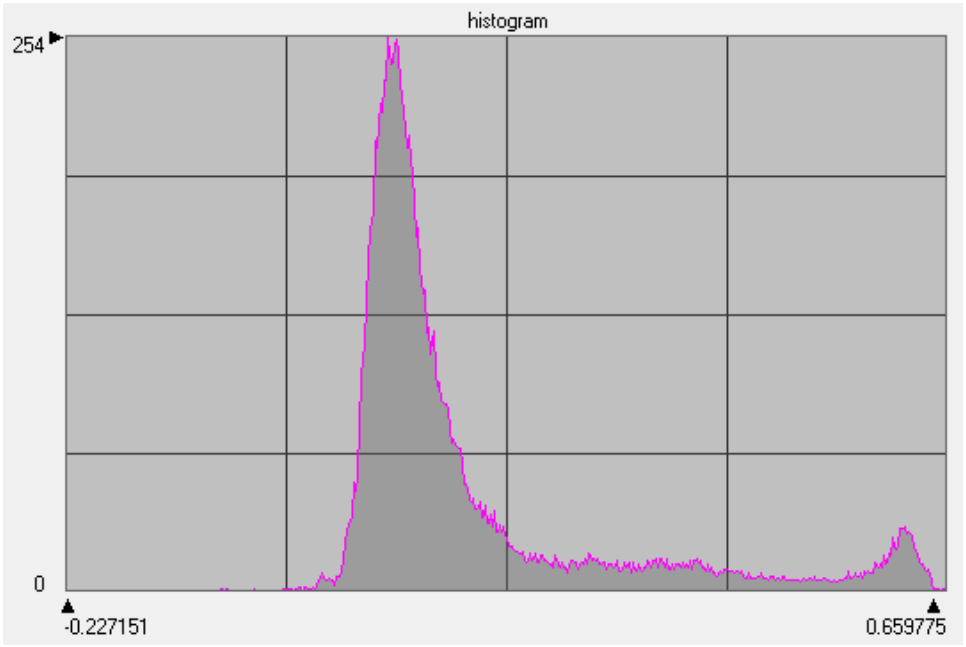

Figure 18: Histogram of NDVI product from September 2018

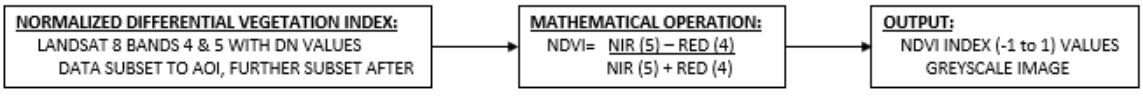

Figure 19: NDVI process flowchart

Conclusion

The Tasseled cap Transformation was initially developed for the original LandSAT MultiSpectral Sensor in 1976 by Kauth and Thomas specifically for agriculture monitoring.[4] This linear transformation increases the separability between vegetation and non-vegetation landcover which allows for determining these and other classes with a high degree of confidence. The process of converting DNs to units of reflectance and correcting for the atmospheric effects was effective in creating comparable datasets. After correction, the range of reflectance values for the agricultural subsets was: May [1.43031], July [1.45566], September [1.409]. This indicates that the highest values and the lowest values varied minimally but the location of the data between these values shifted as the crops matured. This is visually evident in the sequence of scatterplots shown below in figure 20.

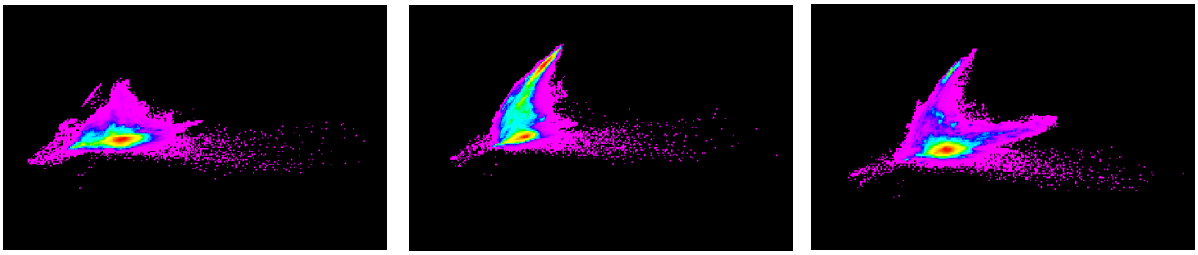

Figure 20: Time series T

The scatterplots above exhibit the typical progression of the combination of brightness and greenness values moving orthogonally from the line of soils parallel to the x axis, up the "cap", and exiting to the right. Unfortunately, the Fall of 2018 happened early and there was snow present in all the imagery from October and November as this effect would have no doubt been exaggerated in the scatterplots.

The NDVI images derived from each month were not taken from the atmospherically corrected datasets and as such are not directly comparable to each other. However, useful information can be gained by examining the results. The image from May is early in the season and is predictably very dark which is indicative of the presence of fallow conditions. The histogram is skewed slightly asymmetrically to the right which is visually represented by the scattering of early season crops. This is evident in both the TCT image as well as the NDVI image shown in figure 21.

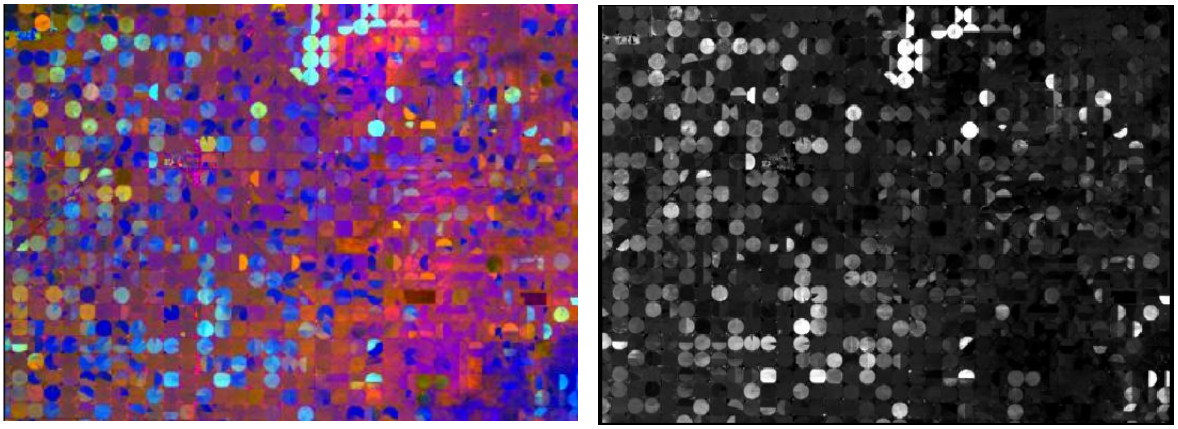

Figure 21: May 2018 TCT and NDVI result.

As the season progressed, the histogram (fig. 16) for the July NDVI image filled out significantly and became strongly bimodal (this trend is also reflected in the histogram for the greenness TCT band). The

increase in vegetation precipitated the overall increase in the statistical mean and mode for the NDVI image from 0.107 & 0.082 in May to 0.36 & 0.62103 in July. The impact of this change is very evident in the images shown in figure 22. Both the TCT and NDVI effectively capture the change in vegetation and display marked increases in overall scene values.

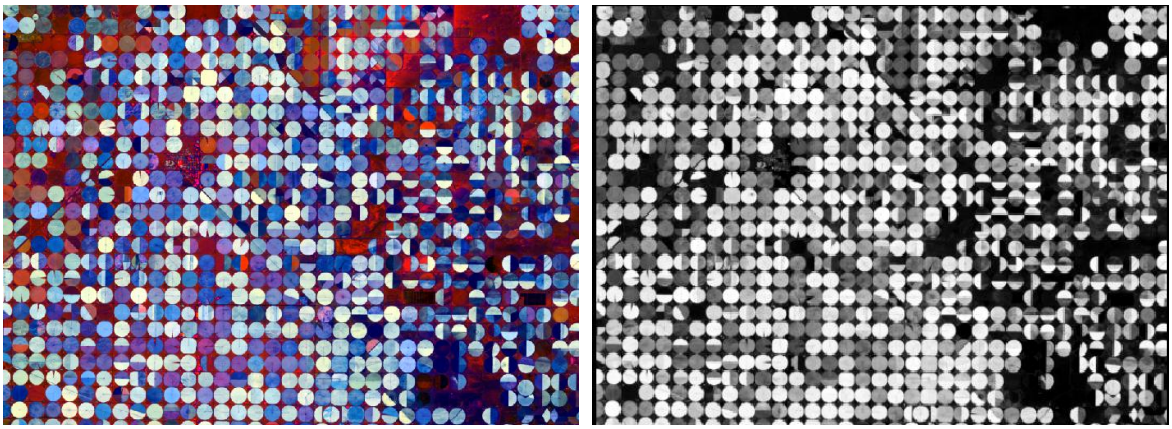

Figure 22: May 2018 TCT and NDVI result.

As the growing season moved into Fall the histogram for the NDVI image maintained its bimodality but the values under the curve deflated, reflecting an overall loss in vegetative land cover. The bimodal nature of the image is most likely due to a late alfalfa crop that the farmer is racing to squeeze in before winter sets in. When displayed side-by-side the TCT and NDVI images display strong visual correlation; however, the response of the NDVI to changes in vegetation status appears to be more finely focused whereas the TCT yields more granular results. Both the images in Figure 23 clearly depict that the potato harvest in the middle of the valley is either well under way or nearing completion and the alfalfa crops on the West (left) side of the image are continuing to photosynthesize the available light. It should be noted that even though the TCT is a fixed model that applies the same weights every time whereas the NDVI relies on the information contained within the image they are both going to be sensitive to any alteration to the initial values.

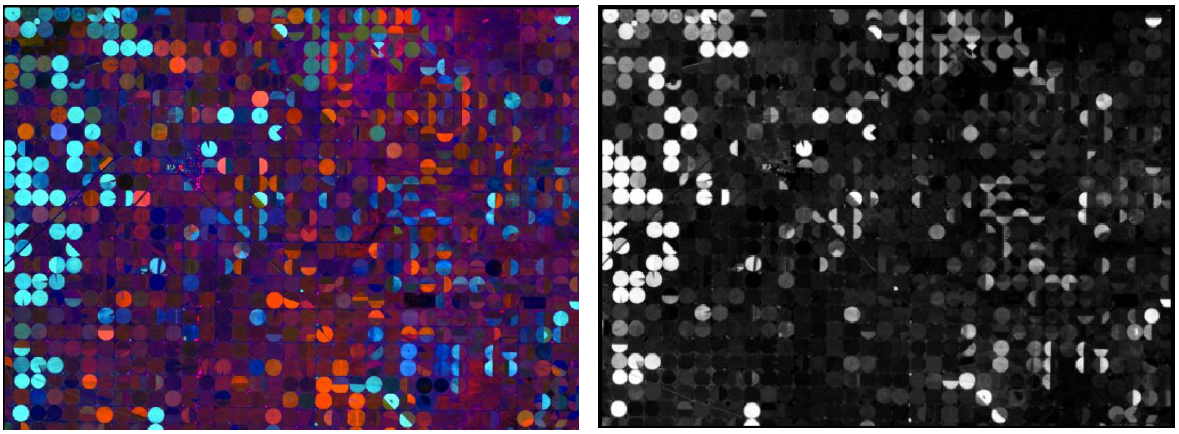

Figure 23: May 2018 TCT and NDVI result.

Both the TCT and NDVI heavily utilized the red and NIR channels, with the NDVI being derived exclusively from these bands and TCT having large coefficients for these channels, so it comes as no

surprise that there is a degree of correlation in the information. Figure 24 illustrates the similarity between the histograms for the measure of greenness provided by the NDVI and the greyscale values for the greenness band of the TCT.

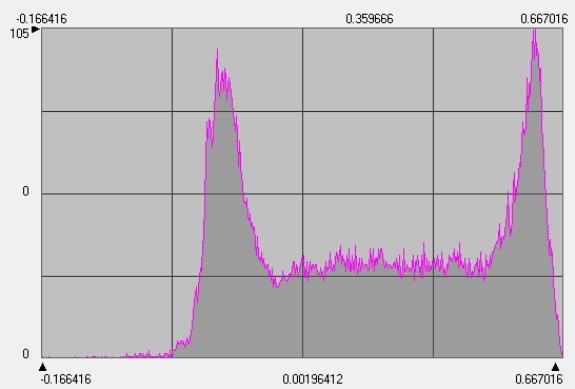

Figure 24: Histograms of NDVI (left) and TCT Greenness band from July 2018

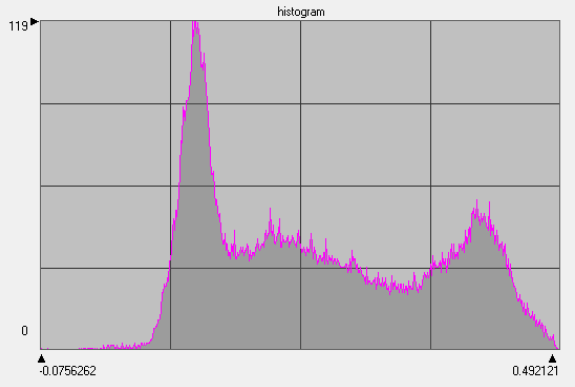

The inverse correlation illustrated in figure 25 demonstrates the relationship between low NDVI values and high TCT brightness values. The fact that there exists a correlation and inverse correlation between two separately derived indices leads me to believe that there may be additional applications of this knowledge to be leveraged in the perpetual search for better results.

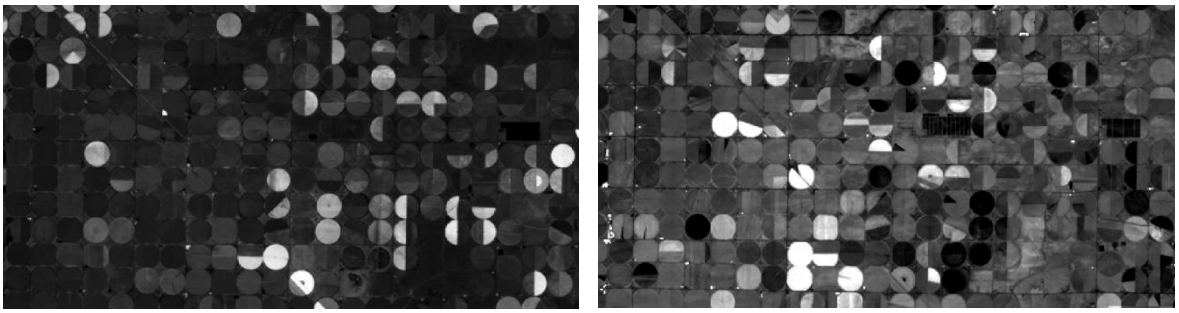

Figure 25: NDVI (l)and TCT Brightness band (r) images from September. Note correlation between low values in NDVI image and high values in TCT Brightness image

Identifying and quantifying vegetation location, type, and health are primary uses for remotely sensed imagery because the information about these attributes directly fuels the decision-making process for many diverse disciplines such as hydrology, land management, ecologic studies, agriculture,

urban planning, and many more. The Tasseled Cap Transformation and the Normalized Difference Vegetation Index are complementary products that are hugely useful for achieving excellent results for vegetation studies. The mathematics underlying each method and physical characteristics of the imaged subject lead me to conclude that the NDVI is more appropriate for larger scale projects that leverage the band ratios to normalize data and the TCT is optimized for agricultural studies as well as providing supplementary information for land cover classification abetted by the multidimensional nature of the output.

References:

1. https://www.usgs.gov/centers/eros/science/usgs-eros-archive-landsat-archives-landsat-8-oli-operational-land-imager-and?qt-science_center_objects=0#qt-science_center_objects

2. Ali, S.M., Salman S.S, (2016). New Tasseled Cap Classification Technique usin LandSAT-8 OLI Image Bands. Iraqui Journal of Science. Vol 57, No. 2C. pp:1612-1619.

3. Anderson, Ian. https://community.hexagongeospatial.com/t5/Spatial-Modeler-Tutorials/Landsat-8-Top-of-Atmosphere-Reflectance-Conversion/ta-p/4223

4. Schowengerdt, Robert A. *Remote Sensing: Models and methods for image processing*. New Delhi: Elsevier, 2011. pp: 337

5. Lillesand, Thomas M., Ralph W. Kiefer, and Jonathan W. Chipman. *Remote sensing and image interpretation*. Hoboken, NJ: John Wiley & Sons, 2008. pp: 535

6. Anderson, Ian. https://community.hexagongeospatial.com/t5/tkb/articleprintpage/tkb-id/KS_SpatialModeler_AnalyticalRecipes/article-id/29

7. Adams, John B., and Alan R. Gillespie. *Remote sensing of landscapes with spectral images: a physical modeling approach*. Cambridge, UK New York: Cambridge University Press, 2006. Print.

8. Ganie, Dr & Asima Nusrath, Dr. (2016). Determining the Vegetation Indices (NDVI) from Landsat 8 Satellite Data. International Journal of Advanced Research. VOL 4. 1459-1463. 10.21474/IJAR01/1348.

Appendix:

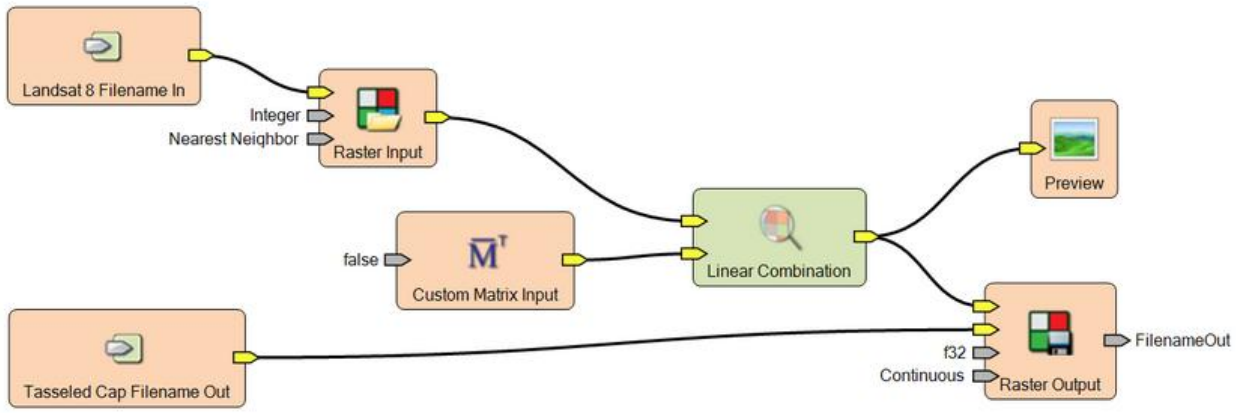

Figure 26:ERDAS Taselled Cap algorithm flowchart for LandSAT-8 OLI data